

YOHKOH/HXT EVIDENCE FOR A HYPERHOT LOOP-TOP SOURCE IN THE PRE-IMPULSIVE PHASE OF A LOOP FLARE

Y. UCHIDA¹, M. S. WHEATLAND², R. HAGA¹, I. YOSHITAKE¹ and D. MELROSE²

¹*Physics Department, Science University of Tokyo, 1-3 Kagurazaka, Shinjuku, Tokyo 162, Japan
(e-mail: uchida@astro1.yy.kagu.sut.ac.jp)*

²*Research Centre for Theoretical Astrophysics, School of Physics, University of Sydney,
NSW 2006, Australia*

(Received 22 September 2000; accepted 8 May 2001)

Abstract. A loop flare that occurred on 22 April 1993 near the disk center is examined using the *Yohkoh* Hard X-ray Telescope (HXT). We specifically looked into the faint early phase of the flare *prior to* the start of the strong impulsive phase. The pre-impulsive phase, though weak in intensity, is expected to contain essential clues to the mechanism of loop flares according to the causality principle, but it has not received attention previously, probably due to the insufficient dynamic range and cadence of observations by the instruments on earlier satellites. Observations with *Yohkoh*/HXT can clarify what occurs in this phase. This flare, like many other flares of this type, shows a relatively weak emission with a smooth and gradual increase during this pre-impulsive phase, followed by impulsive bursts, and then turns into a smooth decay phase without impulsive bursts. First, we found that the spectrum for the initial smooth rise part is consistent with a thin-thermal source at a temperature around 80 MK. Imaging of this phase in the HXT/L and M bands shows a single source between the footpoint sources that will come up in the impulsive phase following this phase, suggesting that this *hyperhot* source is located at a high part of the loop between the footpoints, since this flare takes a form of a loop. Furthermore, as we go up to the earliest times of the flare *before* this ‘hyperhot’ source phase, two fainter sources are found near the footpoint sources that will appear later in the impulsive phase. The spectra of these sources at this earliest time of the flare, in contrast to the ‘hyperhot’ source, cannot be determined from the HXT because the instrument was not in flare mode, and HXT/M1, M2, and H-band data are, unfortunately, not available at this very initial time. We can guess, however, that they are also of thermal character because the time profile is smooth without any spikes just as in the following ‘hyperhot’ thermal phase, and in the post-impulsive ‘superhot’ thermal phase coming up much later. These findings suggest that there is an important, and probably dynamic, early phase in loop flares that has been unnoticed in the still dark pre-impulsive phase, because the very early footpoint sources change into the loop top source in a matter of 20–30 s, comparable to the dynamic Alfvén time scale. Some implications of our new findings are discussed.

1. Introduction

Imaging observations in soft X-rays led to the classification of flares into compact and large-scale arcade-type events (Pallavicini, Serio, and Vaiana, 1977). Compact flares (loop flares) are basically confined to a magnetic loop, whereas arcade flares involve an extended magnetic reconfiguration, and are associated with dark filament eruptions and coronal mass ejections (CME’s). This basic division of flare



types has motivated different theoretical models for each. Although there exists a claim that both might have similar physical process (e.g., Shibata *et al.*, 1995), we here take the standpoint that these two classes are different.

Compact loop flares are characterized by strong impulsive hard X-ray emission that is widely believed to be produced by a population of mildly relativistic particles accelerated in the corona. The particles propagate along magnetic field lines from the source somewhere in the corona down to the chromosphere, where they produce hard X-rays by thick-target bremsstrahlung (a widely accepted theory is by electron bombardment (Brown, 1971; Brown, Spicer, and Melrose, 1979), but a non-standard view by considering protons is claimed by some researchers (Simnett, 1995; Emslie *et al.*, 2000)). This has been confirmed by observation: e.g., hard X-ray images of the impulsive phase of loop flares observed with the *Yohkoh* Hard X-ray Telescope (HXT) typically involve double footpoint sources which brighten almost simultaneously (Sakao, 1994). Also, some flares show thermal soft X-ray emission at loop footpoints that closely matches the impulsive hard X-ray emission (Hudson *et al.*, 1994), which may be a direct signature of heating by high-energy particle bombardment at the footpoints in that phase.

There is also a so-called *superhot* (by contrast with the soft X-ray loop formed later with lower temperature around 15–20 MK) thermal source at the loop top in the hard X-ray emission from loop flares that appears in the late (but earlier than the soft X-ray loop top phase) gradual phase in the hard X-ray burst, as identified from high-resolution hard X-ray observations (Lin and Schwartz, 1987). This component has been reported to have a temperature of 30 MK or so, with an emission measure around 10^{48} cm^{-3} .

The sources we found and report in the present paper, as the results of our investigation of *the faint early phases prior to the strong impulsive phase*, are clearly different from those components well known thus far. Namely, we report here evidence for a *hyperhot thermal source* with a temperature of 80 MK or more in the still faint *pre-impulsive* phase of a loop flare. Furthermore, we found that this ‘hyperhot’ loop top source is *preceded* by a pair of footpoint sources of probably thermal character. Both the *hyperhot* loop top source, and the footpoint sources before that, are newly discovered components suggesting the presence of a very important process in the initial phase of loop flares, not noted thus far. This initial phase is probably very dynamic, since the configuration of the source changes in a matter of 20–30 s, comparable to the dynamic Alfvén transit time scale, and therefore, our findings reported here may affect the previous interpretations of loop flares considerably.

In Section 2 we start with a description of our analysis, and then in Section 3, we show how this loop flare evolved in time. The implications of the observed results are briefly discussed in Section 4. Finally, general discussion is given in Section 5.

2. HXT Data

The solar flare described here is listed in the GOES catalogue as occurring between 14:04 and 14:17 UT on 22 April 1993 in NOAA 7477 seen nearly from its top (the active region at that time was located close to disk center, at N11 E04). The flare was classified M1.5 in the GOES designation. This flare has previously been studied by Gopalswamy *et al.* (1995) using a combination of *Yohkoh* and Very Large Array (VLA) observations, and by Sato (in preparation) by spectral analyses at the intensity maximum phase.

2.1. TIME PROFILES IN DIFFERENT BANDS

The HXT went into flare mode at 14:07:46 UT, and began to accumulate counts in the four energy bands of the instrument while only the L-band was taking data before the flare flag was turned on. The bands and their nominal ranges are L (13.9–22.7 keV), M1 (22.7–32.7 keV), M2 (32.7–52.7 keV), and H (52.7–92.8 keV). (For a complete description of the instrument and its operation, the reader is referred to Kosugi *et al.*, 1991.) Figure 1 shows the count rates in the HXT energy bands for the duration of the flare.

We note in the present paper the part in the very initial phase before the start of the strong impulsive bursts. This weak initial part, having a smooth rising intensity without any spiky features just like the smooth declining slope of the later ‘superhot thermal phase’ of the flare, has not been given special attention before. This was probably due to insufficient dynamic range and cadence of observations in previous satellites, and due to a presumption that the impulsive phase is the first thing of all in loop flares.

We examine the spectra, images, etc. of this pre-impulsive phase in this flare. We take four typical time intervals along the time profiles of the flare as examples in its overall evolution in time, as indicated in Figure 1.

Before discussing these, we briefly mention how we derive them from the HXT data.

2.2. SPECTRAL ANALYSIS

First we consider the problem of fitting the observed spectra from HXT by comparing with the emission from power-law and thin-thermal model emitters.

The instrumental response of the HXT may be described by the probability, $p_i(\varepsilon)$, that a photon with energy ε will be detected in the i th HXT energy bands ($i = 0, 1, 2, 3$, where $i = 0$ denotes the L band, etc.). The functions $p_i(\varepsilon)$ are plotted in the *Yohkoh* HXT Image Catalogue (Sato *et al.*, 1998), and are available in tabulated form as part of the standard SolarSoftWare (Freedland and Handy, 1998) HXT distribution.

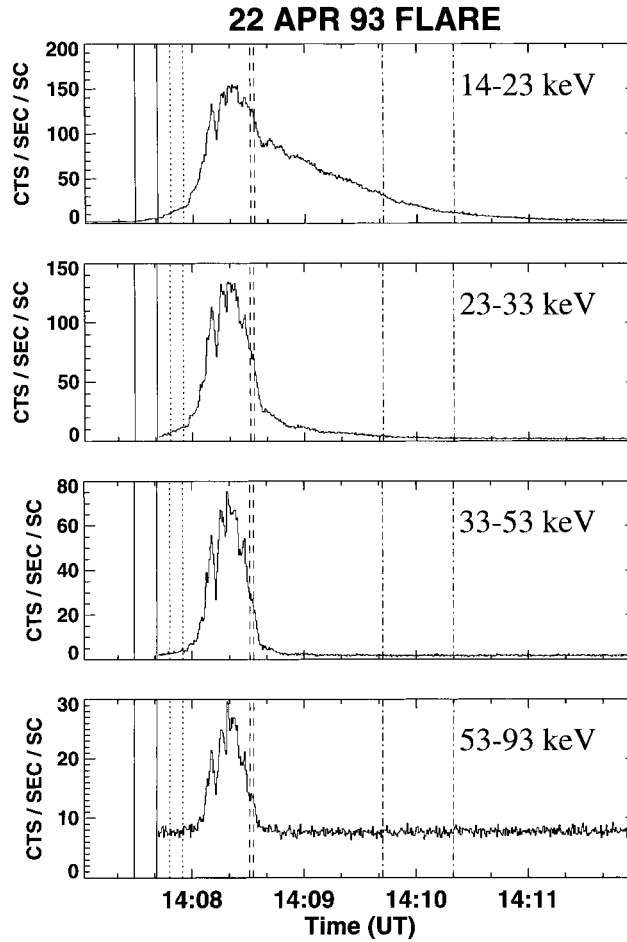


Figure 1. Time profiles in L, M1, and H-bands, of HXT of the loop flare of 22 April 1993: the pairs of vertical lines indicate the time interval I through IV in the text.

Consider an incident photon spectrum $I(\varepsilon)$, in photons per second, per unit energy, and per unit area at the spacecraft. Then the total counts C_i recorded by the HXT band i in an observing period Δt will be

$$C_i = A_{\text{eff}} \Delta t \int_0^{\infty} p_i(\varepsilon) I(\varepsilon) d\varepsilon + B_i, \quad (1)$$

where $A_{\text{eff}} = 57.4 \text{ cm}^2$ is the effective area of the HXT, and B_i represents background counts.

If the incident spectrum is produced by an optically thin isothermal plasma then it depends on the temperature, T , and emission measure M of the emitting material, i.e., $I(\varepsilon) = I(\varepsilon, T, M)$.

Incident isothermal spectra were calculated using the `MEWE_SPEC` routine from the SolarSoftWare distribution, which incorporates continuum and line emission, using the Meyer (1985) solar abundances. In the energy range of interest ($\gtrsim 14$ keV), the dominant contribution to thermal emission is thermal bremsstrahlung. The predicted HXT counts, C_i , were calculated by performing the integral in Equation (1), using the tabulated values of $p_i(\varepsilon)$, and using an estimate of B_i based on background count rates recorded after the flare.

Equation (2) gives the predicted HXT spectrum, for an assumed isothermal incident spectrum. This may be compared with the observed count rate, C_i^{obs} , to determine the emission measure and temperature of a model source which best represents the observed spectrum. A recommended procedure (e.g., Lampton, Margon, and Bowyer, 1976) involves minimizing the chi-square statistic

$$\chi^2 = \sum_{i=0}^3 \frac{(C_i - C_i^{\text{obs}})^2}{C_i}. \quad (2)$$

Minimization of chi-square was achieved via the downhill simplex method (Press *et al.*, 1992). This spectral-fitting procedure was performed for the typical selected time periods during the flare.

It is important to note that the spectral-fitting routine described here incorporates Poisson counting errors (through the denominator of Equation (2)), but does not take into account a number of possible systematic errors. These include errors in HXT gain calibration, modulation error, mis-estimation of background, possible contributions to the L channel from lower-temperature flare plasma, and other instrumental factors. It is difficult to estimate the influence of these factors, and so they are neglected in this simple treatment. Nevertheless, it is important to keep in mind their possible influence.

A similar procedure is performed for the case of a power-law spectrum.

2.3. IMAGING OF SOURCE CONFIGURATION

Although the appearance of this flare in hard X-ray was addressed by Gopalswamy *et al.* (1995), they left out the very initial phases on which we focus our attention here. Also, the calibration of the HXT, and the imaging software for the instrument, have been improved after their work (Sato, Kosugi, and Makishima, 1999).

The HXT is a Fourier synthesis type imaging instrument. Counts are accumulated in 64 bi-grid modulation subcollimators, each having a different pitch and/or position angle for the collimator grids. Photons passing through a single subcollimator are periodically modulated with respect to incident angle, and the count rate data obtained by the detector behind the grids can be regarded as a spatial Fourier component of a hard X-ray image. Hard X-ray images are synthesized from the subcollimator count rates using an image restoration procedure with the maximum entropy method.

In this paper, images were constructed for the typical selected time intervals using the standard `HXTPRO_NMP` routine from the SolarSoftWare HXT distribution.

3. Time Evolution of Spectra and Images

3.1. FOUR TIME INTERVALS IN DIFFERENT PHASES

We first define the four phases in the time development of the 22 April 1993 event as follows: phase A before the flare flag at 14:07:46 UT, phase B between this and the start of the impulsive spike bursts at around 14:08:00, phase C between 14:08:00 and the end of the impulsive spike bursts at around 14:08:40 UT, and phase D, the phase of slow decline after that. In these phases, we choose four typical time intervals representative of the phases in order to show the temporal evolution of the spectra, and source configurations, during the flare.

We select suitable time intervals in each of the phases as follows: We first take a time interval 14:08:31–14:08:33 UT in the impulsive phase (phase C), and label them as time intervals III. Next we adopt a time interval 14:09:42–14:10:20 UT and label it as time interval IV in the so-called ‘superhot thermal phase’ (phase D) sufficiently long after the impulsive spike bursts have ceased. These phases C and D are familiar from the past observations, and we do not go into their details. We have them here only for comparison with the following new results.

Now, in the present paper, we are particularly interested in the weak pre-impulsive phase (phases A and B) prior to 14:08 UT. We take a time interval II, at 14:07:48.5–14:07:54.5 UT, in the smoothly-rising pre-impulsive phase, B, in order to look into what takes place immediately before the impulsive phase. The start of this phase B is the time when HXT went into flare mode.

We further tried to examine the earlier phase A before the flare flag, as allowed. As the result of trials, we decided to take a time interval 14:07:29.5–14:07:41.5 UT, and call it time interval I.

The time profiles of the flare in L, M1, M2, and H bands, together with these selected time intervals are shown in Figure 1.

We show the images of the sources in each time interval in Figure 2(I-a), where I refers to the time intervals I to IV. The observed hard X-ray spectra, together with the best fitted spectral model for each, will be shown in Figure 2(I-b) (and 2(I-c) where applicable), and discussed below.

3.1.1. Time Interval I

The image in Figure 2(I-a) clearly shows that the emission comes from two point sources, the left one is stronger. The right one is weak, but it is sufficiently above the noise level in the L-band, and the persistence of these two sources was confirmed by shifting the time interval to earlier and later times in the same phase. The distance between the centers of the two sources is roughly 1.73×10^4 km projected on the solar surface.

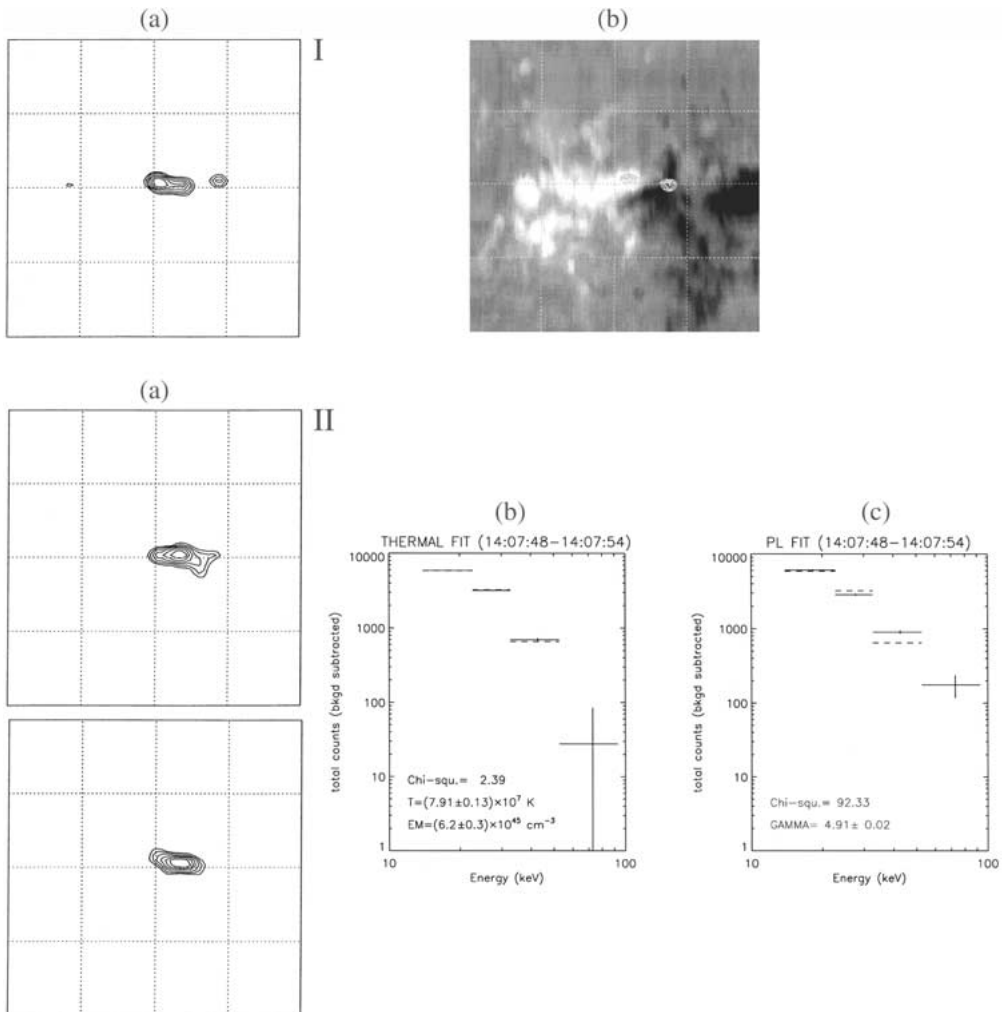


Figure 2A. Time-development of images (left column (a)) for the time intervals I and II. I-a and II-a (upper one) are images in the L-band, and II-a' (lower one) is the image in the M1-band. (Right column (b)) is the Kitt Peak magnetogram for the time of the flare, and (b) and (c) are the IIB and IIC spectral fittings by a thin-thermal, and by power-law model spectra, respectively. It is seen clearly that the source shape was a double in the beginning (I), the source turns into a loop-top single source in the pre-impulsive phase (II) right before the impulsive phase shown in Figure 2(B) on the next page.

Because the HXT went into flare mode at 14:07:46 UT, there are no counts measured in the channels M1, M2, and H prior to this time, and therefore, unfortunately, no spectral information is available for this particular time interval I. We, however, may guess that the sources are likely to be thermal because the time profile in the L-band in this phase is smoothly rising without any spiky components, just like the time profile the later superhot thermal phase (phase D).

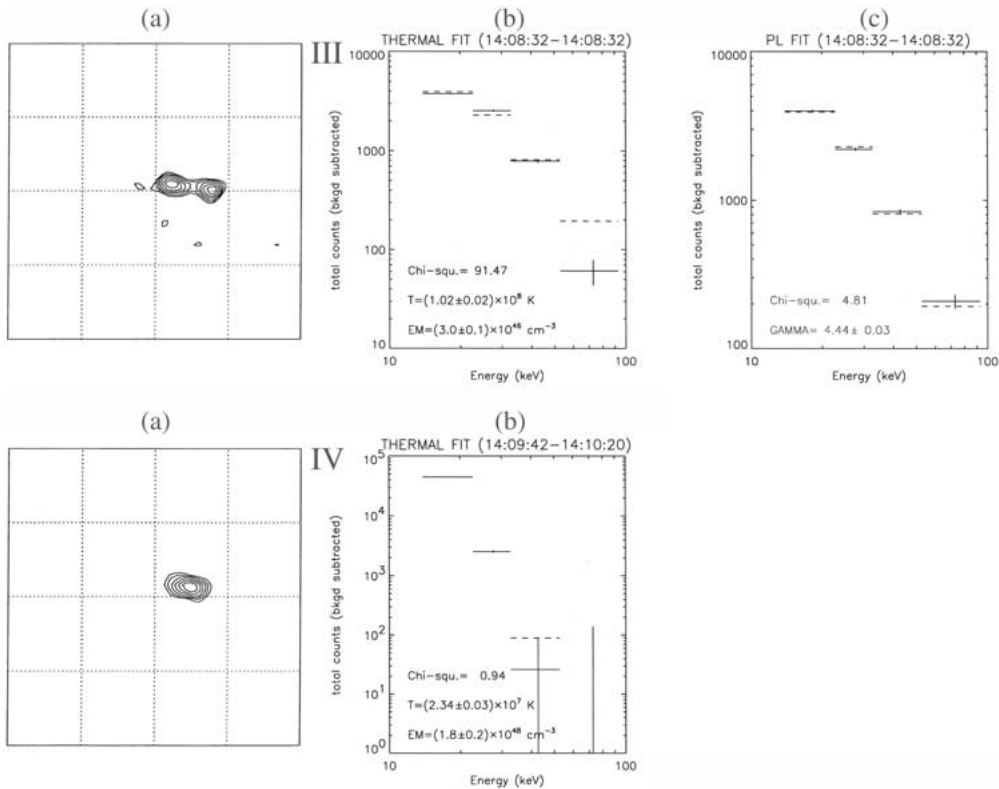


Figure 2B. Time development of images (left column (a)) for the time intervals III and IV. III-a and IV-a are images in the L-band. III-b and IV-b are the spectra fitted by a thin-thermal model, and III-c is fitted by a power-law model spectrum. The source shape is double at the impulsive phase (III), but returns to a single in the ‘super hot thermal’ phase.

3.1.2. Time Interval II

The images in Figure 2(II-a) show clearly that the source of L and M1 bands at this stage is a *single* source midway between the two sources obtained at the time interval I, though somewhat closer to the left-hand-side source.

Since the sources in phases A through D are confined in a narrow elongated region connecting opposite polarity magnetic regions (see Kitt Peak magnetogram including the time of the entire flare, Figure 2(I-b)), it is natural to consider that this is a loop flare (Gopalswamy *et al.*, 1995). This means that a source between the two footpoints is at a high part of the loop.

Figure 2(II-b) shows the HXT spectral fitting by a thin thermal model for time interval II (14:07:48–14:07:54 UT). The dashed horizontal lines in the figure are the (back-ground-subtracted) observed counts in the four HXT energy bands, and the solid horizontal lines represent the counts predicted from the optically thin isothermal model spectrum that provides the best fit to the data. Approximate error bars have been included in the figure, although they are only visible for the two

lowest-energy channels. The value of the chi-square statistic is 2.39, and the probability of obtaining a larger value of chi-square, assuming the model is correct, is 0.35. Hence the isothermal model can be said to provide a good fit to the data for time interval II. The best-fit temperature is $T = (7.91 \pm 0.13) \times 10^7$ K and the corresponding emission measure is $M = (6.2 \pm 0.3) \times 10^{45}$ cm⁻³. The quoted uncertainties are one-sigma estimates, based on the local shape of the χ^2 surface (Press *et al.*, 1992).

Power-law model fitting was also made, and shown in Figure 2(II-c), but the fitting by the power-law spectrum was clearly much poorer ($\chi^2 = 92.3$ with $\gamma = 4.91 \pm 0.02$), and this indicates clearly that the source is thermal.

3.1.3. *Time Interval III*

The image and spectral fitting were made in the time intervals III (14:08:31–14:08:33 UT), a typical part during the impulsive phase, but avoiding the time of strongest spikes in the middle of the impulsive phase C. The reason why we avoided the strongest part in the impulsive phase was due to a kind of ‘saturation’ signature we noted in the strongest spikes. This is not due to instrumental saturation, since there are many other stronger loop type flares with ‘unsaturated’ spikes (Sakao *et al.*, 1998; Sato, 2000), and this interesting feature will be discussed in a separate paper.

In this phase C of strong impulsive bursts, we preferred to show images in the M2-band in order to avoid this ‘saturation’ effect in the L-band. It is seen in Figure 2(III-a) that the image shows double footpoint sources as established before for impulsive bursts (Sakao, 1994).

A point attracting special attention is that the separation between the two footpoint sources here is about 1.65×10^4 km projected on the solar surface, and a bit narrower than that of the sources in time interval I. We give some discussion on this in Section 3.1.5.

Figures 2(III-b) and 2(III-c) show the spectral fittings for the time interval III (14:08:32–14:08:32.5 UT). A fitting by a power-law spectrum gives a much better fit ($\chi^2 = 4.81$ with $\gamma = 4.4 \pm 0.03$) than a thermal fit ($\chi^2 = 91.5$), and the power-law fitting will be adopted here.

3.1.4. *Time Interval IV*

The image in Figure 2(IV-a) tells that the source in time interval IV (14:09:42–14:10:20 UT) is clearly a loop top source between the two sources in the time interval III, consistent with the interpretation that the so-called ‘superhot’ source is a loop top source.

Figure 2(IV-b) show the spectra for the time interval IV (14:09:42–14:10:20.5 UT) in the decaying phase. A good fit to a thermal spectrum is obtained ($\chi^2 = 0.94$, with a probability of a larger value, assuming the model is true, of 0.31). The parameters of the fit are $T = (2.34 \pm 0.03) \times 10^7$ K and the emission measure $M = (1.8 \pm 0.2) \times 10^{48}$ cm⁻³. The inferred temperature is slightly larger

than the temperatures obtained for this time period from soft X-ray measurements (Gopalswamy *et al.*, 1995), and the emission measure is comparable to the soft X-ray emission measures at this time given by them.

3.1.5. *Cross Comparison of the Features in Different Time Intervals*

That the newly discovered source in the pre-impulsive phase, the time interval II, turns out to be a single source between the footpoint sources in the time intervals III as well as those of interval I, and the spectrum is clearly a thermal spectrum with a temperature as high as 80 MK. The finding of such a ‘hyperhot’ source created at a high part of the loop *prior to* the impulsive bursts, is a very exciting finding.

We say that the source was ‘created’, because there was no such a source before that time, and instead, there were two footpoint sources that are likely to be thermal. The locations of these very early double sources at the time interval I are slightly outside of the footpoint sources of the impulsive bursts that come up later. This difference may be explained if the shape of the loop is more than half a circle standing above the photosphere, and if the initial thermal source had a certain height filling the part of the legs, directed away from each other extending from the photospheric footpoints, while the non-thermal bremsstrahlung in phase C comes from the footpoints themselves. There may also be an additional effect since the coexistence of the hyperhot loop top source with the footpoint sources of impulsive bursts may cause certain shifts of the centroids towards the loop-top source.

4. Implication of the Results Obtained

These new results suggest that there is a ‘hyperhot’ (of the order of 80 MK, or higher, but less pronounced when it coexist with the brighter footpoint sources) thermal phase with a single loop top source which was thus far *unnoticed* in the pre-impulsive phase. This has not been noted before partly because of the insufficient dynamic range and cadence of the observations by the previous satellites, but partly because of the prevailing prejudices that the impulsive phase was the very first thing occurring in loop flares. It is also found that there were two weak (thermal) sources near the footpoints at the very beginning of the flare before this ‘hyperhot’ phase. These findings are very important findings concerning the physical process taking place in loop flares *before* the impulsive phase.

The results tell us that (thermal) X-ray sources appear at the very beginning of the flare at the two footpoints of the loop, and then, 20 s or so later, a hyperhot single thermal source appears at a high part of the loop. The strong impulsive (non-thermal) sources at both footpoints *come only after this!* When the strong non-thermal footpoint sources cease, a loop-top ‘superhot’ (30 MK) thermal source remains at the high part of the loop near where the ‘hyperhot’ source existed. It is highly likely that the loop top thermal source existed all the time, cooled from 80 MK (*or higher* during the time of impulsive bursts, but cannot be seen because

the footpoint sources are brighter) down to 30 MK or lower during the 2 min or so time separating intervals II and IV.

It should be noted that the source appears at the loop top, 20–30 s (a time consistent with the Alfvén crossing time across the half of this flare loop) after the pair of thermal-like sources appear at the footpoints. This suggests that the process was highly dynamical. The temperature of the loop-top source as high as 80 MK is likely to be the initial part of the possibly hotter loop-top source being created in this dynamical process. The time of traverse across the length of the loop by high-energy electrons is a few seconds, and so the delay in the appearance of the impulsive burst after the start of these thermal sources should mean that the release of high-energy particles was actually retarded from the initial appearance of these thermal sources. It is, therefore, reasonable to think that the high-energy particles result from the highly dynamical process preceding the impulsive phase.

The above results remind us of the recent proposal by Miyagoshi *et al.* (2000) of an MHD model of loop flares. The model is based on the idea that the active region corona is the dumping ground of magnetic twists (MHD currents) produced in the convection zone under the photosphere (not by the photospheric motion) probably in the twisting up of the magnetic flux tubes in the convective overturn. The active region loop brightenings (Shimizu *et al.*, 1992) may be the heated mass injected in this disposal process of the magnetic twists (Uchida *et al.*, 2000). During the emergence into the coronal magnetic loop from below the photosphere, the twist packets pinch the flux tube and heat the gas near the footpoints, and drive up the gas at near the Alfvén velocity (Uchida and Shibata, 1985).

Miyagoshi *et al.* (2000) proposed with their 3D MHD simulations that a loop flare may result if two twist packets happen to enter into one and the same loop from both sides nearly simultaneously (one of them comes up while the other one from the opposite footpoint is still propagating along the loop) (Uchida and Shibata, 1988; Melrose, 1995; Uchida *et al.*, 1999). This eventuality has a rather small probability per unit time, proportional to the square of the already small probability per unit time of an active region loop brightening on a specific magnetic flux tube in an active region (Wheatland and Uchida, 1999). Heated material driven by the magnetic twist packets collides in the high part of the loop, and a hyperhot source may be produced in the shock in such a collision of two magnetically-driven hypersonic jets.

This process may explain the appearance of thermal sources at the loop footpoints during the earliest times of the flare studied here together with the creation of the loop top ‘hyperhot’ source 20–30 s later. High-energy particles may be accelerated in this model between the two approaching magnetic twist packets by the first-order Fermi mechanism, and the accelerated particles can leak toward the footpoints as the result of the collision of the magnetic twist packets unwinding each other’s twists. This explains the difference in the arrival times between the higher and lower energy particles to the footpoints that Aschwanden and Schwartz

(1996) tried to attribute to the distance to the unseen accelerating source above the loop top.

5. Summary and Discussions

The main result of this paper is to report observation of a ‘hyperhot’ source (since the temperature is much higher than the so-called ‘superhot’ source known before) in the pre-impulsive phase of the 22 April 1993 flare. The observed hard X-ray emission is consistent with that from a thermal plasma at a temperature as high as 80 MK located at a high part of the loop. The finding of the footpoint sources 20–30 s before that suggests that the ‘hyperhot’ loop top source may be created dynamically by some dynamical agents (magnetic twist packets driving pinch-heated gas in our view) coming up from the footpoints.

It is possible, and likely, that the same ‘hyperhot’ source continues to exist with an even higher temperature, and even greater emission measure, than what has been derived in Section 3.1.2, also at the peak time of the impulsive phase. It remains visible after the impulsive phase ceased, as a lower-temperature ‘superhot’ source at the loop-top location. Its presence has not been noted thus far in the impulsive phase due to the presence of brighter impulsive bursts occurring at the footpoints. This is, however, suggested from our imaging of the impulsive phase in different bands, like the narrower width of the footpoints in the L-band than higher bands, and we will report the result in a following paper.

Our ‘hyperhot’ loop-top source reminds us of an earlier report by Takakura (1993). He described that footpoint sources were preceded by a loop-top source. He discussed this by the down-propagation of thermal conduction fronts. We here believe a particle bombardment process because the impulsiveness of the spike bursts and the power-law spectrum are difficult to explain by thermal conduction.

Another interesting point to investigate further is the relation of our ‘hyperhot’ loop-top source with the ‘over-the-loop-top’ source found by Masuda *et al.* (1994). There seems to be an indication that the Masuda source comes a bit earlier than the footpoint sources (Masuda, 1996; Alexander and Metcalf, 1997). Our tentative view is that Masuda’s source might be the same as ours (Miyagoshi *et al.*, 2000), and then the Masuda’s source should come from below, not from above as considered before by assuming an unseen reconnection site in the above (Aschwanden and Schwartz, 1996). The delay of lower energy electrons from higher energy electrons attributed by them to the distance to the high-lying reconnection point (*assumed* even for loop flares) is more naturally explained in our model by the unwinding of the magnetic twists after collision. Namely, the magnetic trap (approaching fast-mode shocks) releases successively higher to lower energy particles (electrons) as the magnetic traps are weakened by mutual unwinding.

The findings reported here should be confirmed by analyses of other loop flares, and we are currently examining the *Yohkoh* catalogue for other events, to see

whether the new hard X-ray component we found is common among loop flares or not. A smooth rise of the intensity in the L-band before the impulsive phase is the characteristic signature of this component. Such a rise seems to exist in many loop flares, but unfortunately, the flare flag of the *Yohkoh* HXT has been set a bit too high to allow us to perform spectral analysis of not very many of the weak initial part of loop flares, but we will be able to examine a few cases to be reported later. We hope that HESSI will be able to provide more cases of this important phase of the loop flare.

Acknowledgements

The authors thank Takeo Kosugi and Hugh Hudson for valuable comments on the draft of this paper. We acknowledge all the *Yohkoh* team members for the successful project. M.S.W. acknowledges the support of a U2000 Post-doctoral Fellowship at the University of Sydney, and of the Japan Society for the Promotion of Science during his two visits to Japan.

References

- Alexander, D. and Metcalf, J.: 1997, *Astrophys. J.* **489**, 442.
 Aschwanden, M. and Schwartz, R.: 1996, *Astrophys. J.* **464**, 974.
 Brown, J.: 1971, *Solar Phys.* **18**, 489.
 Brown, J. C., Spicer, D. S., and Melrose, D. B.: 1979, *Astrophys. J.* **228**, 592.
 Emslie, A. G., Miller, J. A., Vogt, E., Héroux, J.-C., and Sahal-Bréchet, S.: 2000, *Astrophys. J.* **542**, 513.
 Freeland, S. L. and Handy, B. N.: 1998, *Solar Phys.* **182**, 497.
 Gopalswamy, N., Raulin, J.-P., Kundu, M. R., Nitta, N., Lemen, J. R., Herrmann, R., Zarro, D., and Kosugi, T.: 1995, *Astrophys. J.* **455**, 715.
 Hudson, H. S. *et al.*: 1994, *Astrophys. J.* **422**, L25.
 Kosugi, T., Makishima, K., Sakao, T., Dotani, T., Ina, M., Kai, K., Masuda, S., Nakajima, H., Ogawara, Y., Sawa, M., and Shibasaki, K.: 1991, *Solar Phys.* **136**, 17.
 Lampton, M., Margon, B., and Bowyer, S.: 1976, *Astrophys. J.* **208**, 177.
 Lin, R. P. and Schwartz, R. A.: 1987, *Astrophys. J.* **312**, 462.
 Lin, R. P., Schwartz, R. A., Pelling, R. M., and Hurley, K. C.: 1981, *Astrophys. J.* **251**, L109.
 Masuda, S., Kosugi, T., Hara, H., Tsuneta, S., and Ogawara, Y.: 1994, *Nature* **371**, 495.
 Masuda, S.: 1996, in R. Bentley and J. Mariska (eds.), *Magnetic Reconnections in the Solar Atmosphere*, ASP Conf. Series No. 111, p. 166.
 Melrose, D.: 1995, *Astrophys. J.* **451**, 391.
 Meyer, J.-P.: 1985, *Astrophys. J. Suppl.* **57**, 173.
 Miyagoshi, T., Uchida, Y., Yabiku, T., Hirose, S., and Cable, S.: 2001, *Publ. Astron. Soc. Japan*, **53**, 341.
 Pallavicini, R., Serio, S., and Vaiana, G. S.: 1977, *Astrophys. J.* **216**, 108.
 Press, W. H., Teukolsky, S. A., Vetterling, W. T., and Flannery, B. P.: 1992, *Numerical Recipes in C, the Art of Scientific Computing*, 2nd ed., Cambridge University Press, Cambridge.
 Sakao, T.: 1994, Ph.D. Thesis, University Tokyo.

- Sakao, T. *et al.*: 1998, *Observational Plasma Astrophysics*, Kluwer Academic Publishers, Dordrecht, Holland, p. 273.
- Sato, J., Kosugi, T., and Makishima, K.: 1999, *Proc. Astron. Soc. Japan* **51**, 127.
- Sato, J., Sawa, M., Masuda, S., Sakao, T., Kosugi, T., and Sekiguchi, H.: 1998, *The Yohkoh HXT Image Catalogue*, Nobeyama Radio Observatory/NAO, Japan.
- Shapiro, P. R. and Moore, R. T.: 1977, *Astrophys. J.* **217**, 621.
- Shibata, K., Masuda, S., Shimojo, M., Hara, H., Yokoyama, T., Nitta, N., Tsuneta, S., and Kosugi, T.: 1995, *Astrophys. J.* **451**, L83.
- Shimizu, T. *et al.*: 1992, *Publ. Astron. Soc. Japan* **44**, L147.
- Simnett, G.: 1995, *Space Sci. Rev.* **73**, 387.
- Takakura, T.: 1993, *Publ. Astron. Soc. Japan* **45**, 737.
- Uchida, Y. and Shibata, K.: 1985, in M. R. Kundu and G. D. Holman (eds.), *Unstable Current Systems and Plasma Instabilities in Astrophysics*, D. Reidel Publ. Co., Dordrecht, Holland, p. 287.
- Uchida, Y. and Shibata, K.: 1988, *Solar Phys.* **116**, 291.
- Uchida, Y., Hirose, S., Morita, S., Torii, M., Tanaka, T., Yabiku, T., Miyagoshi, T., Uemura, S., and Yamaguchi, T.: 1999, *Astrophys. Space Sci.* **264**, 145.
- Uchida, Y., Miyagoshi, T., Yabiku, T., Cable, S., and Hirose, S.: 2001, *Publ. Astron. Soc. Japan* **53**, 331.
- Wheatland, M. S. and Uchida, Y.: 1999, *Solar Phys.* **189**, 163.